REMARKS

Status of the Claims

1. Claims 26, 29, 30, 39, and 41 are currently amended.

2. Claims 31-38, and 43 are withdrawn.

3. Claims 44-54 are cancelled without prejudice to filing one or more divisional applications.

4. Claims 55-61 are new.

5. Claims 26, 29, 30, 39 and 55-63 are pending examination in this application.

Claim Objections

The Examiner objected to claims 31-36 and 43 as encompassing non-elected subject matter. The Applicant respectfully disagrees. Claims 31-36 and 43 are subject to Examiner's prior requirement for **species election** and do not require restriction or amendment. However, in the interest of clarity and simplicity, Applicant has withdrawn claims 31-36 and 43 and added new claims 56-60 that are drawn to only the <u>elected species</u> of the objected claims. Applicant reserves the right and respectfully requests that the claims withdrawn as a result of this objection be rejoined for further examination if and when the new claims are deemed allowable. Applicant also notes that, following restriction, the subject matter of claims 26 and 29 were identical. Applicant has amended Claim 26 to refer to the measurement of the <u>total</u> amount of Aβ variant whereas Claim 29 has been amended to refer to the detection of one or more Aβ variants. Applicant believes that the matter is within the elected subject matter following restriction and election. New claims 56-60 added in response to the current objection now depend from Claim 29.

The species election of N-terminal truncated β-amyloid at start position 4 (previously in claims 31,32,and 33) now reads on claims 56, 58, and 60; Claims 26 and 29 are generic thereto. The species election of the molecule Aβ (4-42) (previously in claim 34) now reads on claim 57; Claims 26, 29, and 56 are generic thereto. The species election of the molecule Aβ (5-42) (previously in claim 43) now reads on claim 60; claim 26 and 29 are generic thereto. The species election of methylation at position 4 (previously in claim 34) now reads on claim 59; Claims 26, 29, and 58 are generic thereto.

8

<u>Claim Rejections</u>

1. Enablement Rejections—35 USC § 112

        a. Claims 26, 29-43

The Examiner rejected claims 26 and 29-43 as failing to comply with the enablement requirement. Specifically, the Examiner stated that "the claims contain subject matter which was not described in the specification in such a way as to enable one skilled in the art to which it pertains, or with which it is most nearly connected, to make and/or use the invention." Applicant respectfully traverses.

The Applicant believes that Examiner has mischaracterized the claimed scope and utility of present invention in paragraph 10 of the Office Action by requiring that the claimed invention unequivocally diagnosis disease associated with β-amyloid (Aβ) formation and/or aggregation.[1] The present invention relates to a method for the early detection of N-terminal truncated forms of β-amyloid which aids in the determination of whether a mammal may be susceptible to or at risk of diseases associated with β-amyloid formation and/or aggregation. N-terminal truncated forms are known to be present in Alzheimer's patients. (See Specification, p. 6 (citing Masters et al., 1985)).

The present invention is directed to <u>an early identification</u> of patients who are at an increased risk of developing diseases associated with β-amyloid formation and/or aggregation. This part of the population may subsequently develop Alzheimer's disease. (See Specification, Table 8). Applicant notes that diagnostic medical tests do not always present a bright line for the presence of a particular disease, especially during the early stages. Certain tests, however, assist a clinician in weighing the probability that a patient may or may not suffer from a particular condition in the future. Positive results in such tests raise a "red flag" for the necessity of follow-up testing, and may also provide a benchmark for administering preventative treatments or suggesting lifestyle changes, when applicable. The present invention provides such a clinical tool. Applicant has amended the claims to reflect this distinction.

---

[1] Applicant notes that the terms "β-amyloid" and "Aβ" have been used interchangeably in the specification and during prosecution. For the sake of clarity, Applicant will use the term β-amyloid when possible; all of the claims have been amended to use the "β-amyloid" terminology.

9

Attached to this response are additional data in the form of illustrations and figures that shows the utility of the claimed invention (See Appendix 1). While this information is not part of the Specification, the enclosures support Applicant's contention that the Specification is enabling and that one of ordinary skill in the art would be able to perform the claimed invention without undue experimentation. In Appendix 1, S0-S10 refers to the stage of amyloid deposits in the brain. A patient with stages S7-S10 is classified as an Alzheimer's patient. The teachings of the current invention aid in determining the stage of disease by allowing detection of truncated forms in early stages, *i.e.*, those preceding Stage S7. The data on the brain analysis shown in Appendix 1 is obtained by using the method described in the patent Specification on pages 51-55 and Figures cited therein. In Figure 4 of the Specification, S0 is control group wherein no truncated forms are detected while S1, S2 and S6 represent early stages of amyloid formation and/or aggregation and S10 represents an Alzheimer's patient.

Although stage S0 represents control group, N-terminal truncated forms are present in some samples of this group. (See Specification, Fig. 4 and Appendix 1). Presence of the N-terminal truncated forms indicates that these patients are susceptible to and at a risk of developing a disease associated with β-amyloid formation and/or aggregation. Further confirmation of these controls (where N-terminal truncated forms were detected) to develop the disease were not determined in this study because the patients were dead. However, Appendix 2 provides data on the correlation between β-amyloid formation and/or aggregation with presence of N-terminal truncated forms at very early stages as described in present invention by detection of N-terminal truncated forms at 4 and 8 kDa (Appendix 2, Fig. 3). Thus, it is clear that the claimed method does provide a simple and efficient tool to aid in determining whether a mammal is susceptible to or at risk of disease associated with β-amyloid formation and/or aggregation.

Applicant further addresses the Examiners comments in paragraph 10 of the Office Action: "Applicant fails to teach how to identify a mammal susceptible to or at risk to develop a disease associated with Aβ formation/aggregation by detecting these modifications". (Office Action pp. 5-6). As described above, the objective of the invention is an aid to early diagnosis of a disease associated with β-amyloid formation/aggregation by

10

detecting the presence or absence of N-terminal truncated forms of β-amyloid. As stated on page 16 of the specification, "these N-terminal and/or post-translationally modified Aβ variants correspond to the infraclinical stages of AD [(Alzheimer's Disease)].... and can thus be considered as the very first pathological species related to the early events of amylodosis". This detection is possible by 2-D electrophoresis analysis (See Specification, Figure 4 and Table 3) and mass spectrometry (See Table 8). The Specification also discloses several other means for detecting the β-amyloid variants at pages 45-51. Through these specifically disclosed and contemplated methods, physicians may screen patient populations to identify those patients that are susceptible to disease, may require further testing, or may benefit from preventative therapies.

The Examiner also wrote: "Applicant also fails to teach how to screen the clearance of Aβ or predict the level of Aβ burden using these modifications." First, to clarify any ambiguity, Applicant notes that the phrase "predict the level of [β-amyloid] burden" is not intend to mean "forecast the level of [β-amyloid] burden". Claim 30 has been amended to use the word "measure" instead of "predict". Next, Examiner's statement raises two points. First, skilled artisans are taught how to screen β-amyloid variants by the methods described in preceding paragraph, namely, 2D-electrophoresis, mass spectrophotometry, and by the disclosed *in vivo* methods. Second, Applicant directs Examiner to Example 2 (Specification, p. 56) and specifically to Figures 5 and 6 and Table 4. This example shows that antibodies directed to specific forms of N-terminal truncated β-amyloid are unique to particular species of variants disclosed in the Specification due to recognition of the N-terminus of the variants. Furthermore, the total amount of β-amyloid species in a given biological sample (as defined on page 41, ll. 5-19 of the Specification) may be determined by an antibody that recognizes an β-amyloid epitope that is closer to the C-terminus of the disclosed variants (*e.g.*, the β-amyloid antibody 21F12 used in Example 3 on p. 55 of the Specification). Thus, a skilled artisan may determine both the total amount of β-amyloid variant in a given patient sample, and the amount and identity of the individual β-amyloid components that comprise the total Aβ pool. The clearance of β-amyloid is measured after the administration of a known β-amyloid variant. Applicant has amended claim 26 to remove the clearance aspect of the

11

invention and added new claim 55 to further clarify what is claimed. Applicant believes that the amendments and the foregoing discussion addresses the Examiner's points.

The Examiner states further that "the disclosures provided by Applicant have not taught how N-terminal truncated Aβ/post-translationally modified Aβ variant is related to clearance of Aβ or Aβ burden in a mammal". This method has been clearly addressed in the specification beginning on the last paragraph of page 19 and continuing to the end of the section on page 21. This section describes a method of administering an N-terminal truncated-containing composition to elicit an immune response in a mammal as described in Tables 4 and 5 of the specification.

The Examiner further argued: "Applicant has not provided any guidance of the correlation between the level of prediction for a disease associated with Aβ formation and the level of detection." Applicant notes that the claimed method as described above requires determination of the mere presence or absence of N-terminal truncated form in the sample. Presence of <u>any</u> N-terminal truncated β-amyloid species is a risk factor for development and progression of the disease (resulting in amyloid formation and/or aggregation). The examiner further states: "It is difficult to envision what level and what kind of N-terminal truncated Aβ can be considered as abnormal...." <u>Any kind</u> and any level of N-terminal truncated β-amyloid is an indication of risk for amyloid formation and/or aggregation. Example 1 of the Specification shows that a wide variety of β-amyloid variants were detected in brain homogenates of Alzheimer' patents. Example 3 shows that increased detection of certain variants in cerebrospinal fluid, namely the $A\beta_{5-42}$ and $A\beta_{8-42}$ species, occurs as Alzheimer's progresses. While certain forms may predominate in early stages of disease, Applicant reiterates that the presence and detection of <u>any</u> of the disclosed variants is significant. Appendix 1 shows different truncated forms. The present invention has elected N-terminal truncated β-amyloid variants truncated at positions 4 and 5. The variant beginning at position 4 has also been detected in the transgenic mice model confirming the early indication of disease (See Appendix 2, Figure 3 showing a western blot as result of using the antibodies (6E10 and 21F12) as described in the present invention).

The examiner also states that "the skilled artisan cannot envision what other species of N-terminal truncated or post-translationally modified variants to detect." Tables 1 and 2 of

12

the Specification provide a complete list of all the possible N-terminal truncated Aβ forms that are subject of the claimed invention. Applicant directs the Examiner to Appendix 1, as evidence that the claimed method may be performed by detecting any N-terminal truncated form of β-amyloid. Appendix 1 shows successful detection of N-terminal truncated forms from 1-42 to 11-42. This data is evidence that the method may be used with any of the N-terminal truncated or post-translationally modified β-amyloid variants.

The Examiner also stated that: "Applicant has not provided any specific information to predict which one of us would develop a disease associated with amyloid formation/aggregation." Applicant also respectfully disagrees with this statement. The specification, in addition to the additional data (Appendix 1 & 2), demonstrates that the presence of N-terminal truncated species may be considered as a factor in forecasting the onset of diseases associated with amyloid formation/aggregation. While detection of low-levels of N-terminal truncated species may not predict whether a patient will develop a related disease with one-hundred percent certainty, such detection may alert a clinician to the need for follow-up testing or may in some instances provide a clue to help determine the cause of undiagnosed symptoms.

Finally, the Examiner stated that "undue experimentation is required for a person of skill in the art to use the invention" applicant disagrees and directs the examiner to the working examples. The detection is made possible through 2-D electrophoresis analysis and mass spectrometry (See Specification, Figure 4 and Table 3).

b. Claims 30 & 39

The Examiner further rejected claims 30, stating: "Applicant fails to disclose how to distinguish the naturally occurring N-terminal truncated Aβ from the exogenous while administering exogenous N-terminal truncated Aβ in a mammal and comparing the amount of N-terminal truncated Aβ from the said mammal with that in a control." Applicant respectfully traverses.

One objective problem to be solved by the invention is to clear the amyloid deposits (which is a mixture of complete β-amyloid (1-42) and N-truncated forms of different sizes). The solution to this problem is provide exogenous application of a N-truncated β-amyloid; the result is obtained by measuring the total pool of β-amyloid deposits using 2-D

13

electrophoresis analysis and mass spectrometry (See Specification, pp. 51-55). As shown in Figures 3 and 4 and Table 3, the presence and concentration of particular β-amyloid variants may be determined. This is also facilitated by the fact that any given N-terminal truncated variant may be uniquely identified using variant-specific antibodies (See Example 2). Following administration of a particular type of exogenous N-terminal truncated Aβ, the result is a significant reduction in the total pool of amyloid deposits. Where one particular truncated type has been administered exogenously, the concentration of the total pool of β-amyloid variants may be determined and the contribution of the administered Aβ to the total measurement may be subtracted. This technique negates the influence of the exogenously added Aβ variant on the measurement taken of the fluid sample. Amended claim 30 and new claim 55 have been reworded to address Examiner's remarks.

Applicant further disagrees with Examiner's assertion that: "Applicant has not provided enough guidance as to whether all N-terminal truncated Aβ are immunogenic and able to elicit an immune response." (Office Action, p. 8). Rabbits (i.e. mammals) were immunized with β-amyloid variants truncated at positions 5, 6, 8, and 9 and the titer values indicate that these truncated peptides are immunogenic. (See Specification, Table 5). Furthermore, the antibodies are specific for a particular form of β-amyloid variant used (See Specification, Figures 6 and 7). Examiner further remarks that "Applicant fails to teach how much increased amount of antibody or reactive T-cells specific for N-terminal truncated Aβ in a mammal can be considered as at risk to develop a disease associated with Aβ-formation/aggregation." As stated above, the detection of any antibodies specific for N-terminal truncated β-amyloid peptides is a significant warning sign for the possible onset or progression of Aβ-related disease.
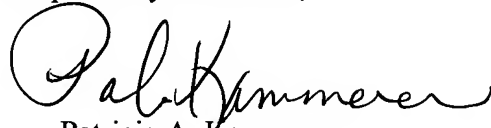
c. **Claims 26, 29, 31-36, 40-43**

The Examiner rejected claims 26, 29, 31-36, 40-43 under 35 USC § 112 ¶ 1 for "being incomplete for omitting essential elements, such omission amounting to a gap between the elements," wherein "The omitted elements are: the controls". The inserted text was inadvertently stricken following the Examiner's restriction requirement. As such, the Applicant believes that the current amendment does not add new matter to the claims. In

14

response, the Applicant has amended claim 26 and its dependent claims to particularly define the controls.

Applicant believes that Examiner's Objections and Rejections have been adequately addressed and overcome through amendment of the claims and the foregoing remarks. The Applicant does not believe that any other fees are due. However, should any additional fees under 37 C.F.R. §§ 1.16 to 1.21 be required for any reason relating to the enclosed materials, the Commissioner is authorized to deduct said fees from Deposit Account No. 08-3038/**11362.0039.NPUS01**. Reconsideration of the application is respectfully requested. Applicant respectfully requests that the claims now be advanced to allowance.

Respectfully submitted,

Patricia A. Kammerer
Reg. No. 29,775
Attorney for Assignee
INNOGENETICS N.V.

Customer No. 23369
HOWREY LLP
1111 Louisiana, 25th Floor
Houston, Texas 77002
(713) 787-1512 (direct)

Date: May 24, 2006

15

Neurobiology

Massive CA1/2 Neuronal Loss with Intraneuronal and N-Terminal Truncated Aβ42 Accumulation in a Novel Alzheimer Transgenic Model

Caty Casas,* Nicolas Sergeant,†
Jean-Michel Itier,‡ Véronique Blanchard,*
Oliver Wirths,§ Nicolien van der Kolk,¶
Valérie Vingtdeux,† Evita van de Steeg,¶
Gwenaëlle Ret,‡ Thierry Canton,* Hervé Drobecq,‖
Allan Clark,‡ Bruno Bonici,* André Delacourte,†
Jesús Benavides,* Christoph Schmitz,¶
Günter Tremp,‡ Thomas A. Bayer,§
Patrick Benoit,* and Laurent Pradier*

*From the Departments of Central Nervous System/Alzheimer
Disease* and Functional Genomics,‡ Aventis-Pharma Paris
Research Center, Vitry sur Seine, France; INSERM U422,† Groupe
Vieillissement Cérébral et Dégénerescence Neuronale. Equipe
Proteomique, Lille, France; UMR8525,‖ Centre National de la
Recherche Scientifique, Institut de Biologie de Lille, Université de
Lille II, Lille, France; the Department of Psychiatry,§ Division of
Neurobiology, Saarland University, Homburg/Saar, Germany;
and the Department of Psychiatry and Neuropsychology,¶
Division of Cellular Neuroscience, Maastricht University,
Maastricht, The Netherlands

Alzheimer's disease (AD) is characterized by a substantial degeneration of pyramidal neurons and the appearance of neuritic plaques and neurofibrillary tangles. Here we present a novel transgenic mouse model, APP^{SL}PS1KI that closely mimics the development of AD-related neuropathological features including a significant hippocampal neuronal loss. This transgenic mouse model carries M233T/L235P knocked-in mutations in presenilin-1 and overexpresses mutated human β-amyloid (Aβ) precursor protein. Aβ$_{x-42}$ is the major form of Aβ species present in this model with progressive development of a complex pattern of N-truncated variants and dimers, similar to those observed in AD brain. At 10 months of age, an extensive neuronal loss (>50%) is present in the CA1/2 hippocampal pyramidal cell layer that correlates with strong accumulation of intraneuronal Aβ and thioflavine-S-positive intracellular material but not with extracellular Aβ deposits. A strong reactive astrogliosis develops together with the neuronal loss. This loss is already detectable at 6 months of age and is

PS1KI gene dosage-dependent. Thus, APP^{SL}PS1KI mice further confirm the critical role of intraneuronal Aβ$_{42}$ in neuronal loss and provide an excellent tool to investigate therapeutic strategies designed to prevent AD neurodegeneration. (Am J Pathol 2004, 165:1289–1300)

Neurodegenerative diseases are morphologically characterized by loss of vulnerable neuronal subpopulations of the central nervous system. Alzheimer's disease (AD) is a progressive neurodegenerative disorder characterized by extensive neuronal degeneration and the development of neuritic amyloid plaques and neurofibrillary tangles. Neuronal and synaptic losses in AD are correlated with dementia and occur in specific brain areas involved in memory processing.[1-3] The core of senile plaques is mainly composed of a heterogeneous amalgam of amyloid-β (Aβ) peptides comprising the full-length, N-terminal truncated, and posttranslationally modified isovariants. Aβ peptides are normally generated by successive proteolysis of the β-amyloid precursor protein (APP), a large transmembrane glycoprotein that is initially cleaved by the β-site APP-cleaving enzyme 1 (BACE1) and subsequently in the transmembrane domain by γ-secretase.[4] The γ-secretase is a multimeric protein complex that includes presenilin (PS), nicastrin, Aph-1, and Pen-2.[5,6] Genetic evidences also support a central role for APP processing in AD neurodegeneration.[7]

Gene-targeted and transgenic mice have proven valuable for modeling various aspects of AD amyloid pathology and associated cognitive changes.[8] However, no mouse model recapitulates the complete human neuropathological spectrum. In particular, there has been little

demonstration of overt neuronal loss in these models,[8] except for the neurons within the volume or in close proximity to Aβ deposits.[9] Using high precision design-based stereological assessment, we have recently characterized a significant neuronal loss in APP^{SL}PS1^{M146L} transgenic mice that occurred in 17-month-old animals.[10] The paucity of neuronal loss in AD transgenic models has been recently reviewed.[11] Here we describe the development of a novel double-transgenic mouse model, APP^{SL}PS1KI carrying four FAD-linked mutations, which develop a massive hippocampal neuronal loss as early as 6 months of age. We first generated a new PS1 knock-in (PS1KI) mouse model carrying the M233T and L235P mutations into the endogenous *presenilin* locus that was then crossed with transgenic APP^{SL} mice.[12] APP^{SL}PS1KI mice develop an accelerated amyloid deposition, as reported for other similar bigenic mice[8] and present a complex pattern of Aβ_{x-42} isovariants highly similar to that described in AD brain.[13] Quite uniquely, APP^{SL}PS1KI mice display an early and massive neuronal loss in the CA1/2 pyramidal cell layer preceded by the presence of abundant intraneuronal Aβ peptide and intracellular thioflavine-S-positive material. Strong astrogliosis also develops in the affected pyramidal layer.

Materials and Methods

Generation of the PS1 Mutant Knock-In Mouse Line

A PS1 knock-in mouse line was derived using a two-step mutagenesis strategy based on the creation of a targeting vector that bears base changes in the coding region at codons M233T and L235P and surrounding introns of the *Ps1* gene,[14,15] as described in Figure 1. Presence of the mutated *Ps1* allele was determined by Southern hybridization of *Eco*RI-restricted genomic DNA with a 230-bp *Ps1* probe indicated in Figure 1A, bottom diagram. Five chimeric mice exhibited germline transmission of the mutant *Ps1* allele. Homozygous (Ho) mice were established and referred to as PS1KI. For gene dosage analysis, PS1KI (He) designates the heterozygous allele. The PS1KI line was established in both pure 129SV and mixed 129SV-C57BL/6 genetic backgrounds and resulted in viable and fertile animals. The mixed PS1KI were bred with APP^{SL} mice, which overexpress human APP$_{751}$ carrying the London (V717I) and Swedish (K670N/M671L) mutations under the control of the Thy1 promoter[12] on a mixed C57BL/6-CBA genetic background. All animals used for this study, including non-transgenic littermate controls, were generated from the same founders (APP^{SL} and PS1KI mice) in two generations and have statistically the same genetic background: C57BL/6 50%-CBA 25%–129SV 25%. When present, the APP transgene was heterozygote.

All experiments on animals were performed in compliance with and following the approval of the Aventis Animal Care and Use Committee, in accordance with standards for the care and use of laboratory animals (Centre National de la Recherche Scientifique-Institute of Laboratory Animal Resources) in accordance with French and European Community rules.

Antibodies

For Western blotting or immunohistochemistry analysis the following primary antibodies were used: anti-PS1, mAb 1563 (Chemicon, Souffelweyersheim, France); anti-tubulin (Sigma, Saint Quentin Fallavier, France); polyclonal rabbit anti-mouse GFAP (DAKO, Glostrup, Denmark), polyclonal antiserum 23850 against APP,[16] anti-serum APP-CTF C17,[17] and rabbit polyclonal antibody against Hspa5 (alias BiP) (SPA-826; Stressgen/TEBU, Perray en Yvelines, France); 6E10 monoclonal antibody directed against human Aβ_{5-15} (Senetek/Biovaley, Marne la Vallée, France) biotinylated 4G8 monoclonal antibody against human Aβ_{17-24} (Senetek); 692 rabbit polyclonal antiserum against human Aβ (generous gift from Gerd Multhaup, Freie Universität Berlin, Berlin, Germany); G2-10 monoclonal antibody to the C-terminus of Aβ_{40} (Genetics Company, Schlieren, Switzerland); 22F9,[18] G2-13 (Genetics Company), and 21F2 (Athena Neurosciences, San Francisco, CA)[13] monoclonal antibodies to the C-terminus of Aβ_{42}.

Western Blot Analysis

Frozen half brains (minus cerebellum) were homogenized in 10 vol of buffer containing 4 mmol/L Tris, pH 7.4, 0.32 mol/L sucrose, and a proteinase inhibitor cocktail (Complete; Roche Diagnostics, Myelan, France). Equal amounts of proteins were separated by sodium dodecyl sulfate-polyacrylamide gel electrophoresis and transferred to nitrocellulose. Membranes were revealed with primary (anti-PS1 C-term or anti-APP C-term) and corresponding horseradish peroxidase-conjugated secondary antibody (New England Biolabs/Ozyme, Montigny, France) followed by enhanced chemiluminescence (Pierce, Asnières, France). Membranes were either exposed to Hyperfilm (Amersham, Saclay, France) or digitalized and analyzed with a GeneGnome 16-bit charge-coupled device video camera and Genetools software (Syngene). The analysis of the full-length and the APP carboxy-terminal fragments (APP-CTFs) was performed, as previously described.[17]

Aβ Electrochemiluminescence Immunoassay

Aβ peptides were detected in brain homogenates by electrochemiluminescence assay using different anti-Aβ antibodies and Origen M8 Analyzer (IGEN Europe Inc.), as previously described.[12] Briefly, the ruthenylated 4G8 antibody (Aβ epitope 17-24) was used in combination with biotinylated 6E10 antibody (Aβ epitope 5-15) to detect total Aβ. To specifically measure Aβ_{x-42} species, the 6E10 antibody was replaced by 22F9. Therefore, the Aβ_{42} assay can detect N-terminal truncated forms of Aβ whereas the total Aβ assay does not.

Two-Dimensional Gel Electrophoresis

Brain homogenates were centrifuged at 100,000 × g for 1 hour at 4°C. The pellet was treated with 1 vol of pure formic acid and sonicated. Formic acid was evaporated under nitrogen and the protein pellet homogenized in two-dimensional lysis buffer (10 mmol/L Tris, 2 mol/L thiourea, 7 mol/L urea, 4% Triton X-100, 20 mmol/L dithiothreitol, 0.4% Pharmalytes, pH 4 to 6.5). Protein concentration was quantified using the 2D Quant protein quantification kit (Amersham). One hundred μg of protein were equilibrated in a ReadyStrip IPG strip, pH 4 to 7 (Bio-Rad, Marnes-la-Coquette, France) and two-dimensional gel electrophoresis and Western blotting were performed, as previously described.[13] Peptide identity was confirmed by mass spectrometry as described,[13] see supplemental Figure S1 available at www.amjpathol.org.

Immunohistochemistry and Histology

Histopathological analysis was in part performed on hemi-brain from single APP[SL] or PS1KI and bigenic mice as well as littermate nontransgenic controls at 2, 6, and 10 months of age (four to eight mice per genotype). Mice were sacrificed by cervical dislocation. After postfixation for 1 week in solution containing 4% paraformaldehyde and 0.1 mol/L phosphate-buffered saline (PBS), pH 7.5, the hemi-brains were stored for 18 hours in PBS containing 20% sucrose and finally frozen at −30°C. Sagittal cryostat floating sections (25 μm thick) were preincubated in blocking buffer (10% normal goat serum in PBS) and then incubated in 0.03% hydrogen peroxide at 19°C for 30 minutes and then in primary antibody solution (biotinylated 4G8 1/200 or anti-Hsap5 1/100). For Hsap5 immunostaining, an incubation (1 hour) with the biotin-coupled anti-rabbit IgG antibody (1/400; Vector Laboratories, Oxford, UK) was performed before incubation with avidin-horseradish peroxidase (Vector Laboratories). Diaminobenzidine tetrahydrochloride was used as a substrate for the peroxidase. Immunostained sections were mounted on chrome-alum-gelatin slides and dehydrated. For Nissl and nucleic acid staining, sections were directly stained for routine histology with cresyl violet (C1791, Sigma) or methyl green (M5015, Sigma).

A different protocol was used for a second group of mice processed for paraffin sections and stereology. Mice were anesthetized and transcardially perfused as described.[10] The right brain halves were postformalin-fixed (immersion fixation in 4% buffered formalin at 4°C) and paraffin-embedded (12 APP[SL], 8 PS1KI, and 12 APP[SL]PS1KI transgenic mice, age and sex matched) and processed according to standard protocols.[18] In brief, 4-μm sections were deparaffinized in xylene and rehydrated. After treatment with 1% H_2O_2 in methanol to block endogenous peroxidase activity, sections were heated in a microwave oven in 0.01 mol/L citrate buffer, pH 6.0. Sections were treated with fetal calf serum before the addition of primary antibodies to block nonspecific binding sites. Incubation of primary antibodies was performed overnight at room temperature. Polyclonal antisera 23850

(1:500, against APP)[16] and 692 (1:500, against Aβ), as well as monoclonal antibodies G2-10 (1:500, against Aβ40) and G2-13 (1:50, against Aβ42) were used as described earlier.[18] Staining was visualized using the ABC method, with a Vectastain kit and diaminobenzidine as chromogen. Double staining was performed in a two-step method. First a conventional staining using the ABC kit (substrate: Vector SG, blue staining) was used, followed by incubation with the second primary antibody and visualization with the ABC method and diaminobenzidine tetrahydrochloride as the chromogen (brown staining). Visualization of aggregated forms of Aβ was performed using 1% thioflavine-S (Sigma, Germany) including 1 μg/ml of 4′,6-diamidine-2′-phenylindole dihydrochloride (Sigma).[19]

Stereological Analysis

Stereological analysis was performed as recently described.[10] Briefly, the left brain halves of the transcardially perfused mice were postfixed in 4% buffered formalin at 4°C and were then cryoprotected by immersion in 30% sucrose in Tris-buffered saline at 4°C overnight. Afterward, brain halves were quickly frozen and stored at −80°C until further processing. Hemi-brains were exhaustively cut into series of 30-μm-thick frontal sections on a cryostat. One series of every tenth section per animal was stained with cresyl violet as described.[10] On all sections showing the hippocampus, the pyramidal cell layer CA1/2 was delineated. Total numbers of neurons were investigated with the Optical Fractionator (Micro Bright Field; Williston, VT). The details of the counting procedure were as follows. Objective used for delineating the pyramidal cell layer CA1–2, ×10; objective used to count the pyramidal cells, ×100; base and height of the unbiased virtual counting spaces used to count neurons, 400 μm^2 and 4 μm, respectively; distance between the unbiased virtual counting spaces in orthogonal directions, x and y, 75 μm; measured actual average section thickness after histological processing, 8.0 μm; average sum of unbiased virtual counting spaces used per animal, 299; average sum of neurons counted per animal, 871; average predicted coefficient of error of the estimated total numbers of neurons, 0.034 (for details see Schmitz and Hof[20]). Differences between groups were tested with analysis of variance followed by posthoc Bonferoni's multiple comparison tests for pairwise comparisons. Statistical significance was established at $P < 0.05$. All calculations were performed using GraphPad Prism version 4.00 for Windows (GraphPad Software, San Diego, CA).

Results

Generation of APP[SL]PS1KI Transgenic Mice and Analysis of APP Metabolism

A PS1 knock-in mouse model carrying two FAD-linked mutations (PS1[M233T] and PS1[L235P]) in the mouse endogenous presenilin-1 gene has been generated (Figure 1).
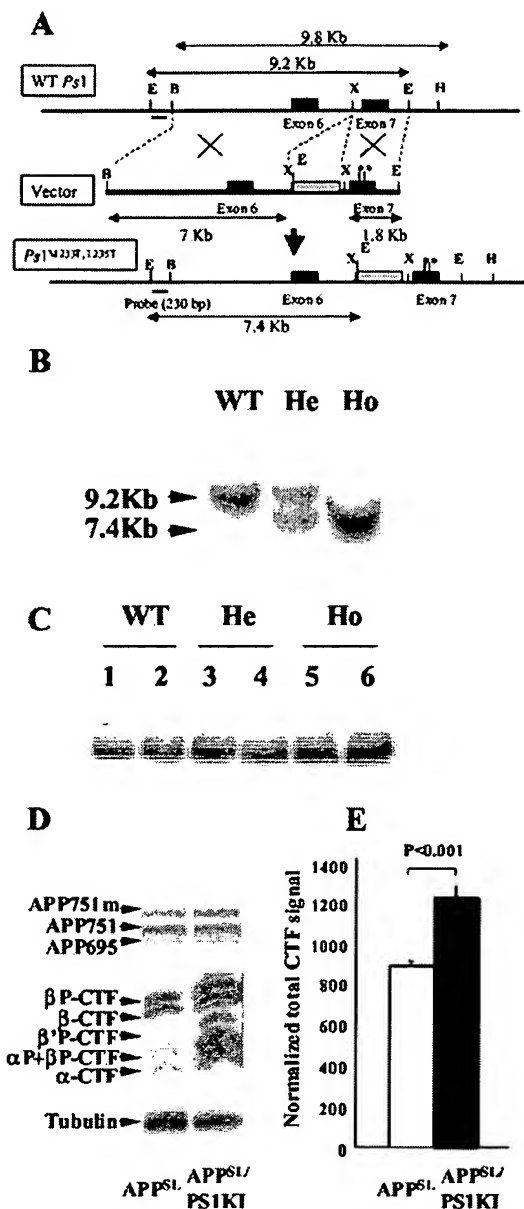
Figure 1. Gene-targeting strategy for PS1KI mouse generation and effect of *Ps1* mutations on PS1 expression and APP metabolism in the mouse brain. **A:** Schematic representation of the structure and restriction map of the wild-type mouse *Ps1* gene (WT *Ps1*) around the exon (**black box**) 7 (**top line**) and the targeting vector used (immediately below **line**, vector) with the neo-cassette (**gray box**). Base pair changes were performed by directed mutagenesis to create M233T and L235P mutations (**) in the exon 7. The modified locus containing the point mutations in *Ps1* gene is illustrated in the **bottom line** (*Ps1^M233T, L235P*). The position of a 230-bp DNA fragment used as a probe for ES cells and mice screening is indicated. Sizes of DNA fragments generated by enzymatic digestion are also indicated. Restriction enzymes: E, *Eco*RI; X, *Xba*I; B, *Bam*HII; H, *Hind*III. **B:** Southern blot hybridization to discriminate among the WT (single 9.2-kb band), homozygous (Ho, single 7.4-kb band), and heterozygous (He, both bands) mice. **C:** Western blot of 20-kd C-terminal PS1 protein showing normal levels in mutant mice. **D:** Analysis of APP holoprotein and APP-CTFs in APP^SL PS1KI mice by Western blot on 6-month-old mouse brain. Detection was performed with APP-CTF C17 antiserum. The three bands detected for the full-length APP correspond to the murine APP₆₉₅ and the immature and mature human APP₇₅₁ isoforms that are not modified. In **middle** panel, **arrows** indicate the α-, β-, β'- and αP-, β'P-, βP-APP-CTFs that are increased in the PS1KI. **E:** Quantification of the Western blot in D was done after signal normalization with tubulin and the value means ± SEM (*n* = 4 mice for each group) obtained for the APP^SL (in white) and APP^SLPS1KI mice (in black) are represented as histograms. Statistical significance was analyzed with the Student's *t*-test.

These mutations were specifically chosen because of their linkage to very early onset FAD at 29 (L235P) and 35 (M233T) years of age.[14,15] Immunoblotting analysis of PS1KI brain extracts established that the expression levels of mouse PS1 C-terminal fragment were not altered by the gene-targeting event (Figure 1C) unlike what was reported in other PS1 knock-in models.[21,22] Breeding the PS1KI mice with an APP^SL transgenic mouse line that overexpress human APP₇₅₁ with Swedish (S) and London (L) mutations,[12,18] generated bigenic mice, APP^SLPS1KI. APP metabolism was analyzed in brain extracts from monogenic and bigenic mice. The introduction of PS1 mutations did not alter the expression levels of the human APP holoprotein (Figure 1D) or soluble sAPPα (data not shown). Analysis of the APP carboxy-terminal fragments (APP-CTFs) identified APP β-, β'-, and α-stubs, as previously reported.[17] After normalization to tubulin levels, we found that the total amount of APP-CTFs was significantly elevated in APP^SLPS1KI compared to APP^SL mice at all ages analyzed (Figure 1, D and E). Thus, the presence of knocked-in PS1^M233T/L235P mutations leads to higher levels of APP-CTFs in the brain of the APP^SLPS1KI mice.

Next, we solubilized all pools of brain Aβ (aggregated, soluble, and membrane raft-associated Aβ) with guanidine hydrochloride and quantified them by an electrochemiluminescence assay. As expected, the presence of PS1 FAD-linked mutations in APP^SLPS1KI mice markedly accelerated Aβ accumulation on aging (Figure 2A), which correlated with the earlier onset of amyloid deposition. Notably, Aβ$_{x-42}$ levels in APP^SLPS1KI mice were extremely high and represented the large majority of Aβ isovariants (Figure 2B). For instance, at the age of 4 months, the ratio of Aβ$_{x-42}$ over total Aβ was 0.85 in APP^SLPS1KI mice compared to a value of 0.3 in APP^SL mice and further increased with age. In young animals (2.5 months and 4 months of age), a gene-dosage effect of the *PS1* mutant allele was apparent on the Aβ$_{x-42}$ accumulation and the Aβ$_{x-42}$/total Aβ ratio. By 10 months of age, total Aβ levels were similar in APP^SL and APP^SLPS1KI mice.
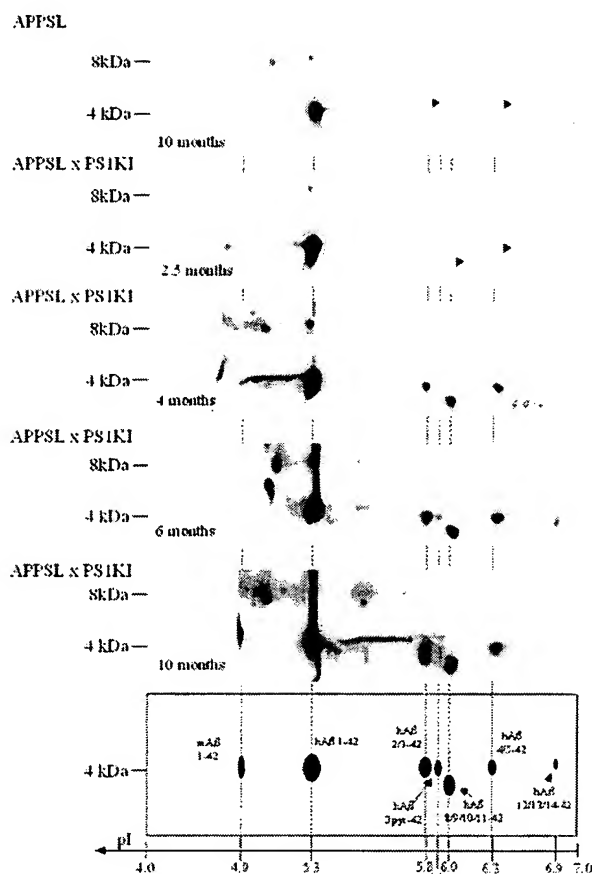
Large Heterogeneity of N-Terminally Truncated Aβ$_{x-42}$ Variants in APP^SLPS1KI Mice

Because the total Aβ quantification assay does not detect most N-truncated forms of Aβ, unlike the Aβ$_{x-42}$ assay, an Aβ$_{x-42}$/total Aβ ratio value greater than unity suggested the presence of N-truncated species. We therefore analyzed the Aβ$_{x-42}$ biochemical characteristics in the APP^SLPS1KI mouse brain using two-dimensional gel electrophoresis.[13] In young bigenic mice (2.5 months of age), the proteomic pattern of Aβ$_{x-42}$ peptides consisted of one major (pI 5.3) and two minor species (pI 6.0 and 6.3) that corresponded to full-length human Aβ$_{1-42}$ (pI 5.3), and N-terminal truncated Aβ$_{x-42}$ forms at positions 8 to 11 (pI 6.0) and at positions 4 or 5 (pI 6.3) (Figure 3). The species identity was confirmed as previously described for human brain Aβ by mass spectrometry (see supplemental Figure S1 available at *www.amjpathol. org*).[13] From the age of 2.5 months onwards, the com-

A

B
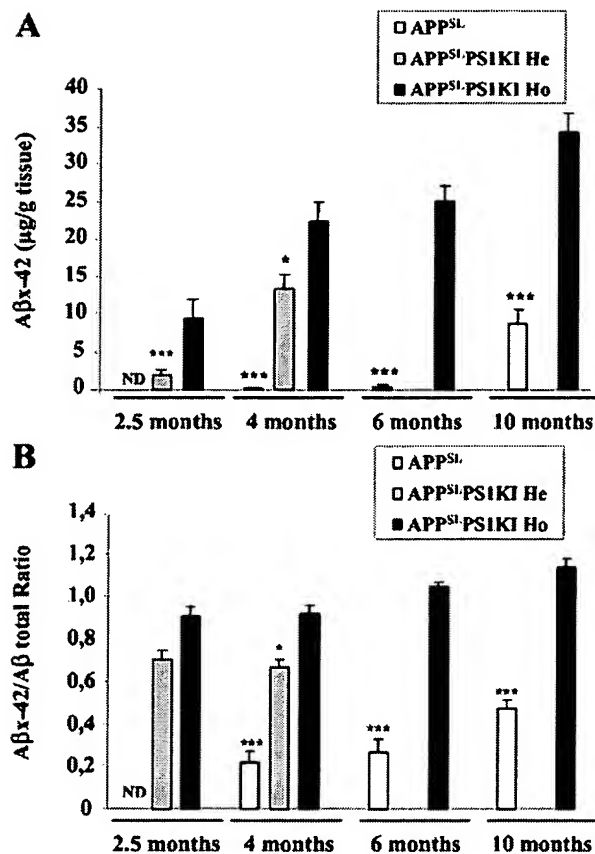
Figure 2. Accelerated Aβ accumulation in APP^{SL}PS1KI mouse brain. Whole brain (minus cerebellum) Aβ$_{42}$ levels (A) or Aβ$_{42}$/total Aβ ratio (B) were quantified by electrochemiluminescence (average ± SEM) in APP^{SL} and APP^{SL}PS1KI homozygous (Ho) or heterozygous (He) for Ps1$^{M233T/L235P}$. Asterisks indicate the significance of the difference whether none, one, or two copies of the mutated PS1 allele are present (*, $P < 0.05$; ***, $P < 0.005$; Mann-Whitney test. $n = 5$ to 7). Note: 6- and 10-month-old hemizygous APP^{SL}PS1KI animals were not investigated.

Figure 3. Proteomic analysis of Aβ$_{42}$ species in the APP^{SL} and APP^{SL}PS1KI transgenic mice. Two-dimensional Western blots of Aβ$_{42}$ species were performed from acid formic-solubilized brain homogenates from APP^{SL} (top) and APP^{SL}PS1KI (remaining panels) transgenic mice at the indicated ages. Two APP^{SL}, one APP^{SL}PS1KI at 2.5 and 4 months of age, and two at 6 and 10 months of age were analyzed. According to the characterization of Aβ$_{42}$ species performed in the human brain of patients with AD[13] and confirmed by mass spectrometry analysis (see supplemental Figure S1), the identity of human Aβ$_{42}$ species (hAβ) is summarized at the bottom. Isoelectric points were determined using internal standards. Spot at pI 4.3 putatively corresponds to the endogenous mouse Aβ$_{42}$ (mAb). Arrowheads point (down leftwards) to the weak staining of spots at pI 5.8 and 6.3. Monomeric species of Aβ$_{42}$ are visualized at 4 kd, whereas dimeric species are resolved at 8 kd.

plexity of the pattern of Aβ isovariants increased with stronger spot intensities and new N-terminal truncated forms progressively appearing. At 4 months of age, an additional spot (pI 5.8) appeared corresponding to human Aβ$_{x-42}$-truncated forms at position 2 and 3. A more acidic Aβ$_{x-42}$ isovariant (pI 4.3) also appeared, which could correspond to mouse Aβ$_{1-42}$. At 6 months of age, we detected additional spots at pI 5.9 and 6.9 corresponding to the pyroglutamate modified N-terminal truncated form of Aβ at position 3 (Aβ$_{N3(pE)}$) and to the Aβ$_{x-42}$ species truncated at positions 12, 13, or 14, respectively (Figure 3). It should be noted that Aβ$_{N3(pE)}$ only appeared 2 months after the corresponding nonmodified Aβ$_{3-42}$ variant. In 10-month-old mice, we observed an identical pattern with stronger intensities. By contrast, in APP^{SL} mouse brain (10 months of age) with the same total Aβ levels as APP^{SL}PS1KI mice, only very limited levels of Aβ$_{42}$ N-terminal truncated isovariants at positions 2, 3, 4, and 5 were detected (Figure 3). We were also able to detect the presence of abundant Aβ dimers (8 kd) resistant to pure formic acid treatment that accumulated in an age-dependent manner in the brain of APP^{SL}PS1KI mice (Figure 3). The presence of heterogeneous N-terminal

truncated isovariants and abundant oligomers in APP^{SL}PS1KI mouse brain closely mimics the situation observed in AD pathology.

Neuronal Loss and Abundant Intracellular Aβ Accumulation in the Brain of APP^{SL}PS1KI Mice

As expected from our biochemical studies, immunohistochemical detection of Aβ peptide using 4G8 antibody confirmed an accelerated rate of Aβ peptide deposition in APP^{SL}PS1KI brain parenchyma. No Aβ deposits were detected in nontransgenic mice or in PS1KI mice. We detected the first signs of Aβ deposition in APP^{SL}PS1KI mouse brain at 2.5 months of age compared to 6 months in APP^{SL} mice as previously described (data not shown).[12] At 6 months, we found widespread and numerous round compact Aβ deposits within the cortical, hippocampa, and thalamic areas of APP^{SL}PS1KI mice whereas in age-matched
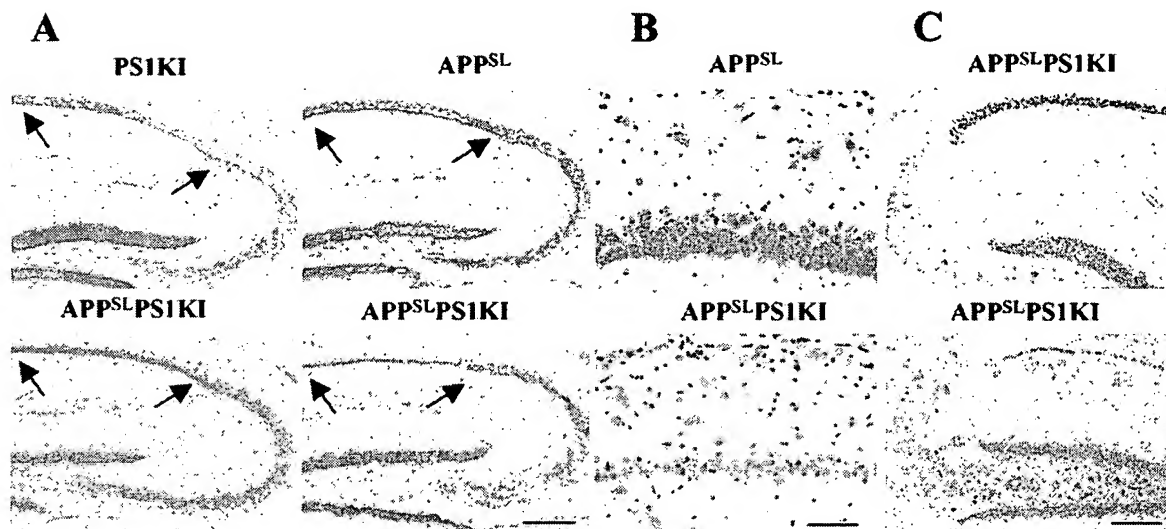
A APP^{SL} APP^{SL}PS1KI
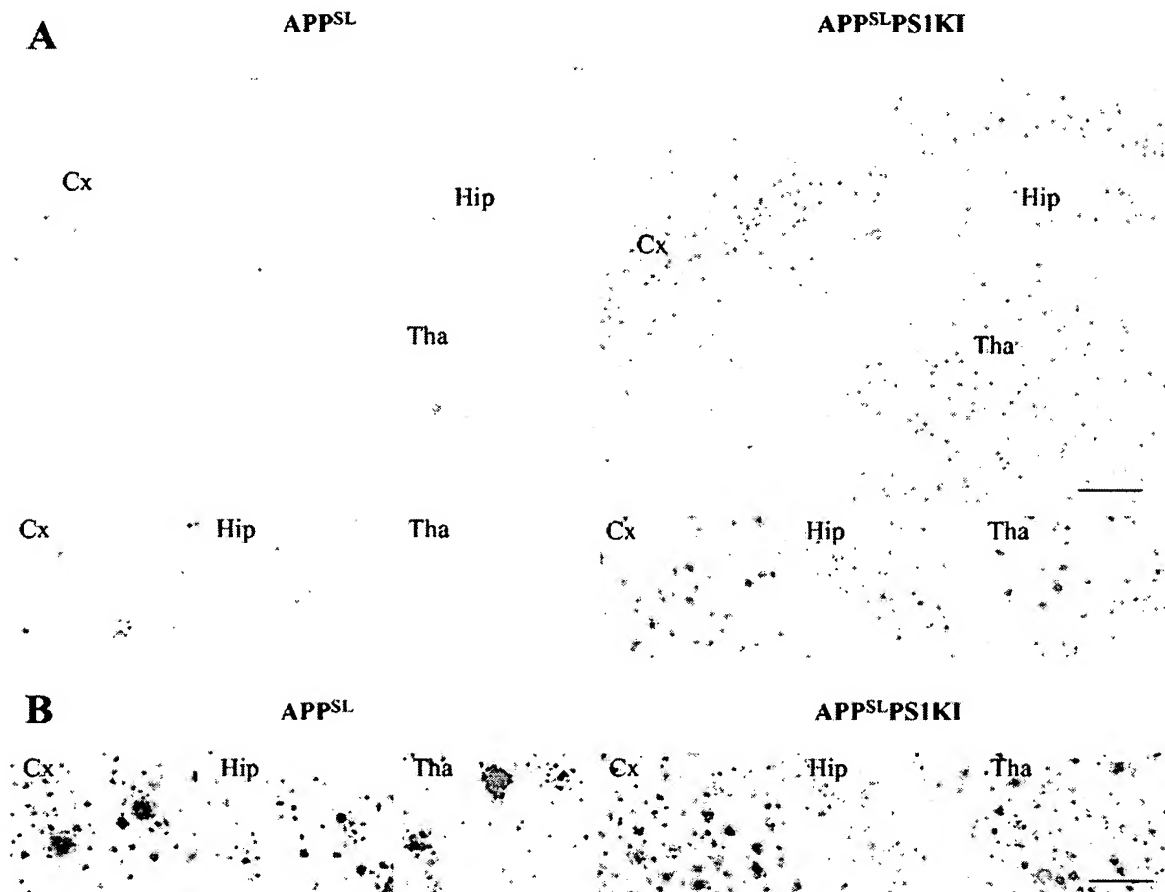
B APP^{SL} APP^{SL}PS1KI

Figure 4. Accelerated Aβ peptide deposition in APP^{SL}PS1KI mouse brain. Representative photomicrographs of Aβ immunostaining on sagittal brain sections taken from 6 (A)- and 10 (B)-month-old APP^{SL} (left) and APP^{SL}PS1KI mice (right) (4G8 antibody on 25-μm-thick cryostat sections). Aβ immunostaining in the entire section and in the cortical (Cx), subicular, hippocampal (Hip), and thalamic (Tha) subareas illustrate the acceleration of extracellular Aβ deposition and its widespread distribution in brain parenchyma of young (ie, 6 months of age) APP^{SL}PS1KI mice (higher magnification in **bottom** panels). Note the difference in the size and number of Aβ deposits in double- versus single-transgenic mice at 10 months of age with overall similar amyloid load (B). Scale bars: 500 μm, **top** panel (A); 20 μm, **middle** panel (A); 20 μm, **bottom** panel (B).

APP^{SL} mice only very few deposits were present and restricted to the subiculum and deeper cortical neuronal layers (Figure 4). In older mice (10 months of age) extracellular Aβ deposit distribution, density, and size were increased in the brains of both models that were reaching similar plaque load. However, we noted differences in the size of Aβ deposits that were more compact, smaller, and more numerous in APP^{SL}PS1KI mice than in APP^{SL} mice (Figure 4B). Similar to other APP transgenic models, astrocytic and microglial activation were present around amyloid plaques (data not shown) together with abundant dystrophic neurites (evidenced by characteristic periplaque APP immunostaining, Figure 5C).

The accelerated Aβ peptide deposition and the presence of abundant $A\beta_{x-42}$ species prompted us to evaluate neuronal survival in APP^{SL}PS1KI mouse brain. Microscopic analysis of cresyl violet-stained brain sections from APP^{SL} or PS1KI mice showed no gross alteration compared to age-matched nontransgenic mice up to 10 months of age (Figure 5A). Strikingly, detailed analysis of the hippocampal CA1-3 subfields and of the dentate gyrus showed that APP^{SL}PS1KI mice developed a marked reduction of the hippocampal pyramidal cell

layer thickness that was particularly prominent in the CA1/2 region at 10 months of age in both males and females (seven of seven bigenic mice, four males and three females; Figure 5, A and B). A marked neuronal loss in 10-month-old APP^{SL}PS1KI mice was also observed with a second histological marker (methyl green dye) and with heat shock protein A5 (Hspa5, alias Bip) immunolabeling (data not shown). APP immunostaining in the brain of 2- and 10-month-old APP^{SL}PS1KI mice further confirmed the age-dependent cell loss in CA1/2 hippocampal subfields (Figure 5C) and indicated that the neuronal loss correlated with a particularly high expression in CA1/2 neurons of the human APP transgene driven by the Thy-promoter (Figure 5C) as previously reported.[18] No overt neuronal loss was observed either in the dentate gyrus or CA3 subfield at this age.

Neuronal loss was quantitatively assessed by high-precision design-based stereology. We found a substantial loss of pyramidal cells within hippocampal layer CA1/2 in 10-month-old APP^{SL}PS1KI mice compared to 2-month-old APP/PS1KI mice (−49%; $P < 0.001$, in both sexes) as well as compared to 2-month-old and 10-month-old APP^{SL} mice [−54% ($P < 0.01$) and −53% ($P <$
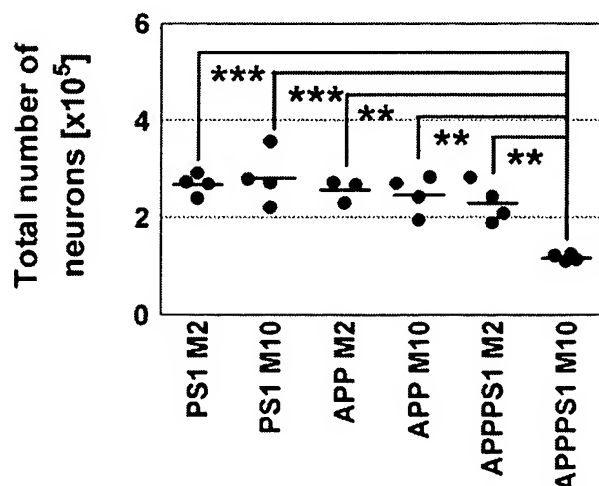
Figure 5. APP^{SL}PS1KI transgenic mice develop massive neuronal loss in the hippocampus. **A:** Representative photomicrographs of cresyl violet-stained sagittal brain sections of 10-month-old PS1KI, APP^{SL}, and two APP^{SL}PS1KI mice at low magnification. Note the deeply reduced thickness of the CA1/2 pyramidal cell layer indicated between **arrows** in the APP^{SL}PS1KI brain (**bottom**). **B:** Higher magnification views of the cresyl violet-stained CA1/2 subfield of a representative APP^{SL} (**top**) and APP^{SL}PS1KI (**bottom**) mouse are shown. **C:** APP immunostaining of the hippocampal formation in 2 (**top**)- and 10 (**bottom**)-month-old APP^{SL}PS1KI mice. APP staining reveals a very strong APP expression in CA1/2 subfield with a faint labeling in CA3 where no neuronal loss was detected. Note again the reduced thickness of CA1/2 subfield with the APP neuronal immunostaining. Scale bars: 150 μm (**A**); 50 μm (**B**); 100 μm (**C**).

0.01), respectively] and compared to 2-month-old and 10-month-old PS1KI mice [−56% ($P < 0.001$) and −59% ($P < 0.001$), respectively; Figure 6]. There was a striking difference between the substantial neuron loss in the hippocampal CA1/2 field (~50%) and the almost lack of amyloid plaques within the CA1/2 pyramidal cell layer.

Interestingly, macroscopic analysis indicated that some CA1/2 neuronal cell loss was present as early as 6 months of age in the brains of APP^{SL}PS1KI female mice ($n = 5$ of 5; see also Figure 8B) but not in three males

Figure 6. Stereological examination of total numbers of neurons within CA1/2 hippocampal cell layer. APP^{SL}, PS1KI, and APP^{SL}PS1KI transgenic were analyzed by high precision design-based stereological assessment (see Material and Methods). M2, 2-month-old animals (PS1KI, four males; APP^{SL}, two males and one female; APP^{SL}PS1KI, two males and two females). M10, 10-month-old animals (PS1KI, four males; APP^{SL}, three males and one female; APP^{SL}PS1KI, two males and two females). Differences between the groups were tested with analysis of variance followed by posthoc Bonferroni's multiple comparison test for pair-wise comparisons. Statistical significance was established at $P < 0.05$. **, $P < 0.01$; ***, $P < 0.001$.
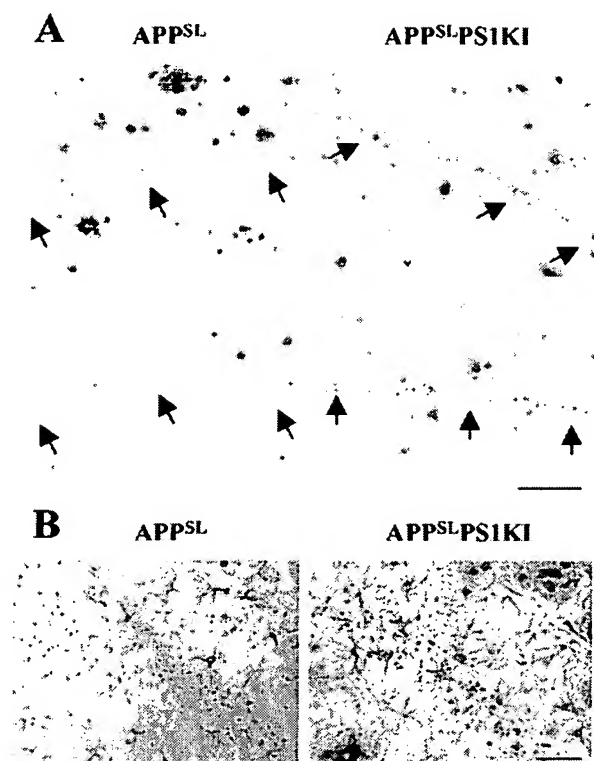
suggesting that females were affected earlier than male mice. Furthermore, the neuronal loss was also observed in 15-month-old APP^{SL}PS1KI heterozygous (He) mice, confirming the existence of a PS1KI gene-dosage effect (data not shown). The disruption of deep cortical layers suggests that the neuronal loss might extend well beyond the CA1/2 region, but further analysis will be necessary to document it throughout the brain.

Analysis of adjacent brain sections stained with Aβ antibodies did not demonstrate an obvious relationship between CA1/2 cell death and extracellular Aβ peptide deposition in APP^{SL}PS1KI mice (Figure 7A and Figure 8). Whereas neuronal loss was observed throughout the entire length of the CA1/2 pyramidal layer, most extracellular Aβ deposits were essentially sparsely distributed on either side of the CA1/2 subfield (ie, in the stratum radiatum, lacunosum-molecular, and oriens) but not within the pyramidal neuronal layer. Moreover, the finding that 10-month-old APP^{SL} mice with, for some, a hippocampal Aβ deposit load quite similar to APP^{SL}PS1KI (Figure 7A, left) did not display neuronal loss in CA1/2 subfield further suggests that cell death in APP^{SL}PS1KI mice is not apparently linked to the deposition of extracellular Aβ peptides. By contrast, the neuronal loss in the CA1/2 region was closely correlated with marked intraneuronal Aβ immunostaining that was present as early as 2 months of age (Figure 7A and Figure 8A). Within the pyramidal neuronal layer, both the density and the intensity of Aβ peptide-immunostained granular bodies were higher in APP^{SL}PS1KI mice compared to APP^{SL} mice (Figure 7A) and much stronger in the CA1/2 subfield in agreement with APP transgene expression. A very significant astrogliosis developed in the area of strong intraneuronal Aβ immunoreactivity and neuronal loss (Figure 7B). High magnification in 4-μm-thin tissue sections using a large array of pan-Aβ (Figure 8; A to C and F) and Aβ$_{40}$ (Figure

Figure 7. Relationship between neuronal loss and intraneuronal Aβ peptide accumulation in the CA1/2 subfield. Representative photomicrographs of Aβ immunostaining (4G8 antibody) on sagittal brain sections of 10-month-old APP^{SL} (left) and APP^{SL}-PS1KI (right) mice. Two different mice per group are illustrated. **A:** Within the CA1/2 hippocampal subarea Aβ deposits are mainly present on either side of rather than within the pyramidal cell layer in both APP^{SL} and APP^{SL}PS1KI. Both the intensity and frequency of granular Aβ immunostaining within the remaining CA1/2 pyramidal cells were increased in APP^{SL}PS1KI mice compared to APP^{SL} mice. **Arrows** indicate the localization of the CA1/2 neuronal cell layer. **B:** Astrocytic staining against GFAP (blue) and Aβ staining (antiserum 692, brown) in CA1 of a 6-month-old APP^{SL} (left) and APP^{SL}PS1KI (right) 4-μm brain sections. Note the astrogliosis in the pyramidal cell layer in APP^{SL}PS1KI mice. Scale bars: 100 μm (A); 50 μm (B).

8H)- or Aβ$_{42}$ (Figure 8I)-specific antibodies demonstrated the Aβ intraneuronal localization within CA1 and subiculum neurons. Double immunostaining with APP and Aβ antibodies indicated the different subcellular localizations of the two markers within neurons (Figure 8G).

Furthermore, thioflavine-S-positive intracellular material could be detected as early as 2 months of age in APP^{SL}PS1KI mice in the CA1/2 region, as well as in the subiculum but not in CA3 or dentate gyrus. In 2-month-old mice, a punctate thioflavine-S staining pattern was detectable, with larger, compact granules in the 10-month-old APP^{SL}PS1KI mice (Figure 8, D and E) whereas neuronal loss was apparent only from 6 months on. Therefore both the granular intraneuronal Aβ immunostaining and the intracellular thioflavine-S-positive material were present as early as 2 months of age, preceding neuronal loss. Both markers were also observed in subiculum and cortical neurons of 2-month-old APP^{SL}PS1KI mice, which further suggests that neuronal loss is also likely to occur in other brain areas but full assessment will require additional analysis. No thioflavine-S staining was detected in APP^{SL}, PS1KI, or nontransgenic control mice.

The APP^{SL}PS1KI transgenic mouse model therefore develops an early neuronal loss within the hippocampal CA1/2 pyramidal cell layer, which correlates with the presence of abundant intraneuronal Aβ peptide and intracellular thioflavine-S-positive material.

Discussion

The generation of transgenic mouse models based on mutant *APP* and *Ps1* genes have enabled major advances in our understanding of the amyloid cascade hypothesis.[23] These models recapitulate several features of AD, including amyloid plaques with dystrophic neurites, synaptic dysfunction and behavioral deficits but fail to develop extensive neuronal death. In view of the much higher sensitivity to Aβ neurotoxicity in older versus younger primates,[24] the lack of neuronal loss in transgenic mice with a high amyloid burden was attributed to their short life span. Here we describe a novel transgenic mouse model, APP^{SL}PS1KI, which carries two PS1 knocked-in and two APP FAD-linked mutations. In addition to the expected acceleration of extracellular Aβ peptide deposition, the APP^{SL}PS1KI model develops an age-dependent massive neuronal loss in the hippocampus, a structure involved in learning and memory processes. Specific neurodegeneration in the hippocampal CA1 subfield and entorhinal cortex is an early event in the AD pathology that correlates directly with the severity of the disease.[1] Interestingly, APP^{SL}PS1KI mice show extensive neuronal loss in the CA1/2 subfield at 10 months of age in both male and female mice with detection as early as 6 months in female mice. In this model, the neuronal loss is definitely biased by the APP transgene expression pattern (very high expression in CA1/2 but not in CA3) but is likely more widely distributed with further aging, especially in subiculum and cortical regions (see below). Additional stereological analysis will be necessary to further document neuronal loss in such areas as entorhinal cortex and other cortical regions. The CA1/2 neuronal loss in APP^{SL}PS1KI mice extends homogeneously throughout the pyramidal layer and is not related to the local proximity of extracellular Aβ peptide deposits. It is therefore distinct from the neuronal loss observed in most other transgenic models, which has been limited to the close vicinity of Aβ deposits.[9] Previously, APP23 transgenic mice were shown to develop a moderate loss of CA1 neurons in older animals (14 to 18 months of age) in close correlation with amyloid plaque load.[25] We have also recently described a significant neuronal loss extending beyond amyloid plaques but less pronounced and again in significantly older (>17 months of age) bigenic APP^{SL}PS1^{M146L} mice using stereological methods.[10,11] By contrast, the early neuronal loss in the present APP^{SL}PS1KI mice is very prominent as early as 6 to 10 months of age. Remarkably, the neuronal loss distribution closely parallels the strong intraneuronal Aβ immunostaining and the accumulation of intracellular thioflavine-S-positive material present throughout the pyramidal cell layer but does not correlate with extracellular deposits. Strong astrogliosis is also occurring in proximity of Aβ-
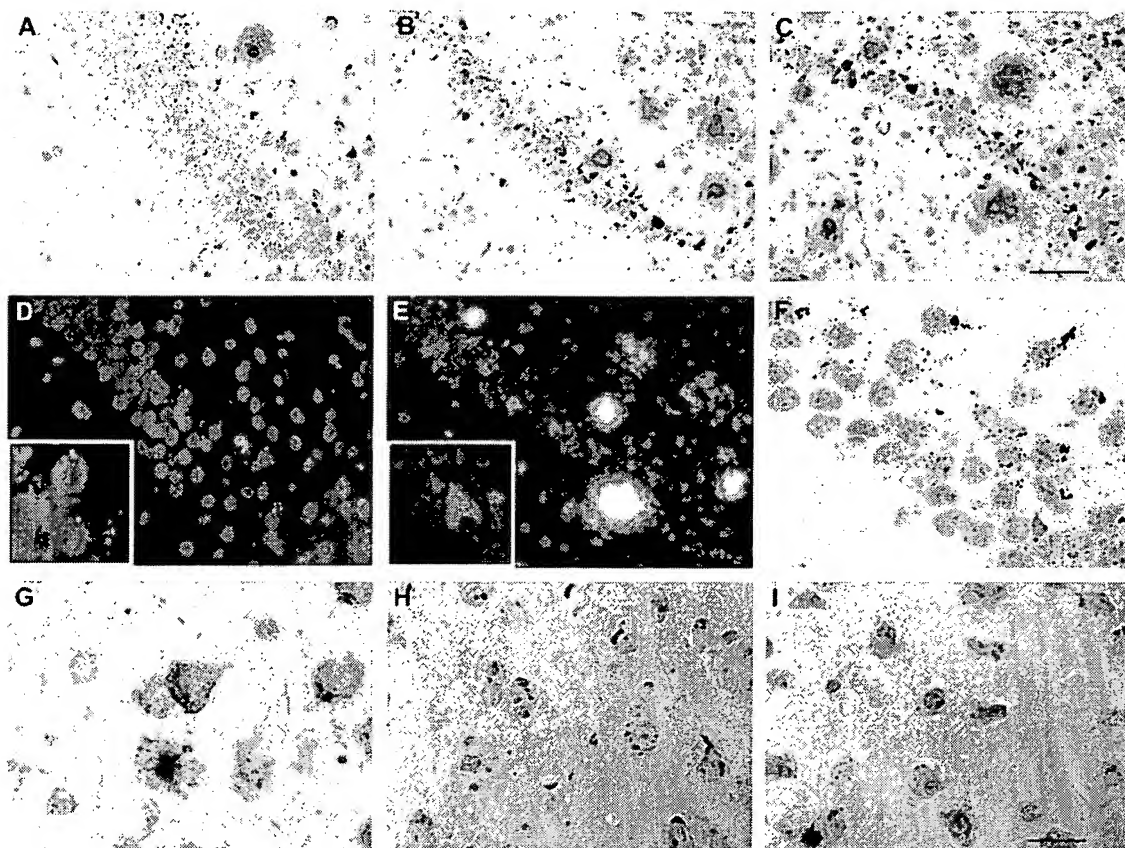
Figure 8. Intraneuronal Aβ peptide accumulation in CA1/2. Representative photomicrographs of Aβ immunoreactivity in 2 (**A**)-, 6 (**B**)-, and 10 (**C**)-month-old APP^{SL}PS1KI mice (antibody 692). Whereas young mice show a punctate staining pattern, larger and compact granules were evident in aged mice. **B:** Note the reduced thickness of the CA1/2 pyramidal layer already at 6 months. **D** and **E:** Thioflavine-S staining reveals aggregated intracellular material in 2 (**D**)- and 10 (**E**)-month-old APP^{SL}PS1KI mice. **F:** High-power photomicrograph demonstrating abundant intraneuronal Aβ in the CA1 subfield of a 2-month-old APP^{SL}PS1KI mouse. **G:** Double labeling of Aβ (blue) and APP (brown) in a 2-month-old APP^{SL}PS1KI mouse, showing abundant intraneuronal Aβ in cortical APP-expressing neurons. **H** and **I:** High-power photomicrographs of the subiculum of a 2-month-old APP^{SL}PS1KI mouse showing abundant intraneuronal Aβ$_{40}$ (**H**) as well as Aβ$_{42}$ (**I**). The thickness of the sections was 4 μm in all pictures. Counter staining was performed with hematoxylin (**A-C**, **F**, **H**, **I**) and 4',6-diamidine-2'-phenylindole dihydrochloride (**D**, **E**). Scale bars: 50 μm (**A–E**); 2 μm (**F–I**). Original magnifications: ×400 (**D**, **E**); ×1000 (insets in **D**, **E**).

positive neurons. Both intraneuronal Aβ and thioflavine-S-positive material stainings preceded neuronal loss. It will be important in future experiments to confirm that the thioflavine-S-positive material is indeed Aβ as suggested by the present results. There is growing evidence that intraneuronal Aβ accumulation is important for the pathogenesis of both AD,[26,27] and Down syndrome,[28,29] with one report of thioflavine-S-positive material in AD.[27] Intraneuronal Aβ accumulation (but not thioflavine-S-positive) has also been documented in several amyloid transgenic mouse models,[12,30–32] including our previous APP^{SL}PS1^{M146L} model, in association with neuronal stress and synaptic alterations. In addition, it has been shown that microinjection of Aβ$_{42}$, but not Aβ$_{40}$, into cultured human primary neurons is drastically more toxic than its extracellular application.[33] As demonstrated by direct Aβ$_{42}$ immunohistochemistry and because Aβ$_{42}$ is the predominant Aβ isovariant produced in APP^{SL}PS1KI mice, the intraneuronal pool of Aβ$_{42}$ in the pyramidal cell layer most likely contributes to the neuronal loss observed, especially if present in an aggregated conformation as suggested by the thioflavine-S staining. Alternatively, Aβ$_{42}$ oligomers are highly abundant in the APP^{SL}PS1KI brain and might also

participate to the CA1/2 neuronal loss in APP^{SL}PS1KI mice. Indeed, Kim and colleagues[34] reported a selective neurotoxicity in the CA1 area and entorhinal cortex promoted by Aβ oligomers or amyloid diffusible ligands. Both the intraneuronal Aβ and the intracellular thioflavine-S stainings extended to cortical regions, strongly suggesting that neuronal loss in other brain areas such as entorhinal cortex could be detected in APP^{SL}PS1KI mice of older age.

Two distinctive biochemical features of the Aβ$_{x-42}$ peptide accumulating in APP^{SL}PS1KI brain could contribute to the observed phenotype. First, it is remarkable that Aβ$_{x-42}$ is the major form accumulated with a ratio of Aβ$_{x-42}$/total Aβ close to 1 compared to a ratio of 0.2 to 0.3 in the APP^{SL} mice. Certainly, this ratio might be slightly overestimated in aged mice because of the presence of N-terminal truncated Aβ species (not detected in the total Aβ assay) observed from 4 months of age onwards, but not in 2.5-month-old mice (ratio value of 0.85). In comparison, the same APP^{SL} mouse line bred with standard overexpressing PS1^{M146L} transgenic mice leads to an Aβ$_{x-42}$/total Aβ ratio of only 0.3 to 0.4,[12] similar to the range of values reported for a large number of other APP-based transgenics, even with PS1 knock-in muta-

tions.[21,35] This might result from the specific combination of double PS1 and APP mutations. In addition, the mutant form of PS1 is expressed at physiological levels by all cells (PS1 knock-in) in the present model unlike some of the previously characterized PS1 knock-in mice that demonstrated a lower expression of the mutant allele.[23,24] Thus, the vast unbalanced mix in favor of $A\beta_{x-42}$ is a key factor for acceleration of $A\beta$ aggregation and would likely contribute to the presence of intracellular thioflavine-S-positive material and the subsequent neuronal toxicity in APP^{SL}PS1KI mice. An additional difference with our previously described bigenic APP^{SL}PS1^{M146L} mice is that the levels of APP C-terminal fragments are increased in APP^{SL}PS1KI whereas they are decreased in APP^{SL}PS1^{M146L} mice (unpublished data). The latter is consistent with the observed large overexpression of mutant PS1^{M146L} fragments (and therefore of γ-secretase activity) whereas in PS1 knock-in mutants, the increase in APP C-terminal fragments could be indicative of a partial loss of γ-secretase activity. Intriguingly, PS1 FAD mutations have also been presented as partial loss-of-function mutations[36] and recently the conditional PS1 knockout transgenic mice has been shown to develop major neuronal loss as in the present report.[37] It is tempting to speculate that in PS1 mutant overexpressing transgenics, the partial loss of function is offset by the large PS1 overexpression leading only to the relative increase in $A\beta_{42}$ but not to neuronal loss. In all instances, the PS1-mutant KI model is by construction a better simulation of the human PS1 mutant FAD.

Another possible contributing factor to neuronal loss in APP^{SL}PS1KI is the presence of a highly heterogeneous population of N-terminal truncated $A\beta_{42}$ forms in brain. Truncated $A\beta$ peptides at the N-terminus are known to aggregate more readily and to accumulate in the brain of sporadic AD patients, in early onset FAD patients, especially in PS1 mutation carriers,[38,39] and in Down syndrome brain.[40–42] The major forms of N-truncated $A\beta$ species in AD senile plaques are those modified by cyclization at residues 3 and 11 with pyroglutamate.[38,43] In APP^{SL}PS1KI mice, N-truncated $A\beta_{42}$ species appearance follows $A\beta_{1-42}$ accumulation with subsequent detection of modified forms, such as $A\beta_{3(pE)}$, at an age with the first signs of hippocampal neuronal loss. The time sequence suggests that $A\beta$ N-terminal truncations and modifications are temporally related to plaque maturation. However, in APP^{SL} mice, with a similar amyloid burden as APP^{SL}PS1KI mice (10 months of age), N-truncated forms of $A\beta$ are far less abundant, indicating that they do not simply result from postdeposition N-terminal exoproteolysis. This data indicates that PS1 mutations not only affect the specificity of the $A\beta$ peptide cleavage at its C-terminus, as part of the γ-secretase complex, but could also alter N-terminus cleavage. We cannot exclude the possibility that N-terminal truncated $A\beta$ forms could result from *de novo* alternative β-cleavages. BACE1 is the main β-secretase cleaving APP at positions 1 or 11 of the $A\beta$ peptide.[44–46] Because interactions between BACE1, PS1, and the γ-secretase complex have been recently reported,[47,48] PS1 mutations could induce, by altering BACE1 selectivity or recruiting

other β-secretases, an array of different truncated $A\beta_{x-42}$ forms, as previously suggested by Russo and colleagues[39] Altogether, the complex pattern of $A\beta$ N-terminal truncated forms in APP^{SL}PS1KI mice closely resembles that found in AD brain[13] and represents the first report of such species in APP-based transgenic models. Because these $A\beta$ species aggregate more readily and are more toxic, they might play a key role in the neurotoxicity observed in this model. The APP^{SL}PS1KI mice could enable a further characterization of the process whereby $A\beta$ truncated forms are generated and a further elucidation of their pathological role.

In summary, APP^{SL}PS1KI is the first transgenic AD model to our knowledge showing early onset and severe neuronal loss. The neuronal loss is correlated with the presence of abundant intraneuronal $A\beta$ and intracellular thioflavine-S-positive material rather than extracellular $A\beta$ deposits. $A\beta_{1-42}$ is the major $A\beta$ form produced in this model with progressive appearance of N-truncated and dimeric species. The present data add further evidence for a pathological role of $A\beta_{42}$ species, especially the $A\beta_{x-42}$ intraneuronal pool, which could therefore represent a prime target for therapeutic intervention. Additionally, the massive neuronal loss observed in an APP-based transgenic model provides a yet-missing link between $A\beta$ peptide and neuronal toxicity *in vivo* in strong support for the $A\beta$ peptide hypothesis of AD, but further highlighting that amyloid plaques might not be a critical factor. The relevance of this multi-FAD mutant transgenic model to sporadic AD remains to be confirmed. However, the major involvement of intraneuronal $A\beta$ has been previously highlighted in AD[26,27] and $A\beta_{42}$ levels are strongly increased after head trauma, a major AD environmental risk factor. Similarly, the N-terminal truncated forms of $A\beta_{42}$ have first been detected in sporadic short-term AD cases.[13] The multiple mutations in the present model are likely critical to recapitulate in a few months a pathological process taking decades in man. In conclusion, APP^{SL}PS1KI mice represent a significant novel AD model and a unique tool to investigate therapeutic strategies designed to prevent AD-related neuronal death.

Acknowledgments

References

1. West MJ, Coleman PD, Flood DG, Troncoso JC: Differences in the pattern of hippocampal neuronal loss in normal ageing and Alzheimer's disease. Lancet 1994, 344:769–772
2. Gomez-Isla T, Price JL, McKeel Jr DW, Morris JC, Growdon JH, Hyman BT: Profound loss of layer II entorhinal cortex neurons occurs in very mild Alzheimer's disease. J Neurosci 1996, 16:4491–4500

3. Morrison JH, Hof PR: Life and death of neurons in the aging brain. Science 1997, 278:412–419

4. Wolfe MS: The secretases of Alzheimer's disease. Curr Top Dev Biol 2003, 54:233–261

5. Francis R, McGrath G, Zhang J, Ruddy DA, Sym M, Apfeld J, Nicoll M, Maxwell M, Hai B, Ellis MC, Parks AL, Xu W, Li J, Gurney M, Myers RL, Himes CS, Hiebsch R, Ruble C, Nye JS, Curtis D: Aph-1 and pen-2 are required for Notch pathway signaling, gamma-secretase cleavage of betaAPP, and presenilin protein accumulation. Dev Cell 2002, 3:85–97

6. Yu G, Nishimura M, Arawaka S, Levitan D, Zhang L, Tandon A, Song YQ, Rogaeva E, Chen F, Kawarai T, Supala A, Levesque L, Yu H, Yang DS, Holmes E, Milman P, Liang Y, Zhang DM, Xu DH, Sato C, Rogaev E, Smith M, Janus C, Zhang Y, Aebersold R, Farrer LS, Sorbi S, Bruni A, Fraser P, St. George-Hyslop P: Nicastrin modulates presenilin-mediated notch/glp-1 signal transduction and betaAPP processing. Nature 2000, 407:48–54

7. Selkoe DJ: Presenilin, Notch, and the genesis and treatment of Alzheimer's disease. Proc Natl Acad Sci USA 2001, 98:11039–11041

8. Higgins GA, Jacobsen H: Transgenic mouse models of Alzheimer's disease: phenotype and application. Behav Pharmacol 2003, 14: 419–438

9. Urbanc B, Cruz L, Le R, Sanders J, Ashe KH, Duff K, Stanley HE, Irizarry MC, Hyman BT: Neurotoxic effects of thioflavin S-positive amyloid deposits in transgenic mice and Alzheimer's disease. Proc Natl Acad Sci USA 2002, 99:13990–13995

10. Schmitz C, Rutten BP, Pielen A, Schafer S, Wirths O, Tremp G, Czech C, Blanchard V, Multhaup G, Rezaie P, Korr H, Steinbusch HWM, Pradier L, Bayer TA: Hippocampal neuron loss exceeds amyloid plaque load in a transgenic mouse model of Alzheimer's disease. Am J Pathol 2004, 164:1495–1502

11. Dickson DW: Building a more perfect beast: APP transgenic mice with neuronal loss. Am J Pathol 2004, 164:1143–1146

12. Blanchard V, Moussaoui S, Czech C, Touchet N, Bonici B, Planche M, Canton T, Jedidi I, Gohin M, Wirths O, Bayer TA, Langui D, Duyckaerts C, Tremp G, Pradier L: Time sequence of maturation of dystrophic neurites associated with Abeta deposits in APP/PS1 transgenic mice. Exp Neurol 2003, 184:247–263

13. Sergeant N, Bombois S, Ghestem A, Drobecq H, Kostanjevecki V, Missiaen C, Wattez A, David JP, Vanmechelen E, Sergheraert C, Delacourte A: Truncated beta-amyloid peptide species in pre-clinical Alzheimer's disease as new targets for the vaccination approach. J Neurochem 2003, 85:1581–1591

14. Kwok JB, Taddei K, Hallupp M, Fisher C, Brooks WS, Broe GA, Hardy J, Fulham MJ, Nicholson GA, Stell R, St. George Hyslop PH, Fraser PE, Kakulas B, Clarnette R, Relkin N, Gandy SE, Schofield PR, Martins RN: Two novel (M233T and R278T) presenilin-1 mutations in early-onset Alzheimer's disease pedigrees and preliminary evidence for association of presenilin-1 mutations with a novel phenotype. Neuroreport 1997, 8:1537–1542

15. Campion D, Brice A, Dumanchin C, Puel M, Baulac M, De La Sayette V, Hannequin D, Duyckaerts C, Michon A, Martin C, Moreau V, Penet C, Martinez M, Clerget-Darpoux F, Agid Y, Frebourg T: A novel presenilin 1 mutation resulting in familial Alzheimer's disease with an onset age of 29 years. Neuroreport 1996, 7:1582–1584

16. Borchardt T, Camakaris J, Cappai R, Masters CL, Beyreuther K, Multhaup G: Copper inhibits beta-amyloid production and stimulates the non-amyloidogenic pathway of amyloid-precursor-protein secretion. Biochem J 1999, 344:461–467

17. Sergeant N, David JP, Champain D, Ghestem A, Wattez A, Delacourte A: Progressive decrease of amyloid precursor protein carboxy terminal fragments (APP-CTFs), associated with tau pathology stages, in Alzheimer's disease. J Neurochem 2002, 81:663–672

18. Wirths O, Multhaup G, Czech C, Feldmann N, Blanchard V, Tremp G, Beyreuther K, Pradier L, Bayer TA: Intraneuronal APP/A beta trafficking and plaque formation in beta-amyloid precursor protein and presenilin-1 transgenic mice. Brain Pathol 2002, 12:275–286

19. Tomidokoro Y, Harigaya Y, Matsubara E, Ikeda M, Kawarabayashi T, Shirao T, Ishiguro K, Okamoto K, Younkin SG, Shoji M: Brain Abeta amyloidosis in APPsw mice induces accumulation of presenilin-1 and tau. J Pathol 2001, 194:500–506

20. Schmitz C, Hof PR: Recommendations for straightforward and rigorous methods of counting neurons based on a computer simulation approach. J Chem Neuroanat 2000, 20:93–114

21. Siman R, Reaume AG, Savage MJ, Trusko S, Lin YG, Scott RW, Flood DG: Presenilin-1 P264L knock-in mutation: differential effects on abeta production, amyloid deposition, and neuronal vulnerability. J Neurosci 2000, 20:8717–8726

22. Rozmahel R, Huang J, Chen F, Liang Y, Nguyen V, Ikeda M, Levesque G, Yu G, Nishimura M, Mathews P, Schmidt SD, Mercken M, Bergeron C, Westaway D, St. George-Hyslop P: Normal brain development in PS1 hypomorphic mice with markedly reduced gamma-secretase cleavage of betaAPP. Neurobiol Aging 2002, 23:187–194

23. Suh YH, Checler F: Amyloid precursor protein, presenilins, and alpha-synuclein: molecular pathogenesis and pharmacological applications in Alzheimer's disease. Pharmacol Rev 2002, 54:469–525

24. Geula C, Wu CK, Saroff D, Lorenzo A, Yuan M, Yankner BA: Aging renders the brain vulnerable to amyloid beta-protein neurotoxicity. Nat Med 1998, 4:827–831

25. Calhoun ME, Wiederhold KH, Abramowski D, Phinney AL, Probst A, Sturchler-Pierrat C, Staufenbiel M, Sommer B, Jucker M: Neuron loss in APP transgenic mice. Nature 1998, 395:755–756

26. Gouras GK, Tsai J, Naslund J, Vincent B, Edgar M, Checler F, Greenfield JP, Haroutunian V, Buxbaum JD, Xu H, Greengard P, Relkin NR: Intraneuronal Abeta42 accumulation in human brain. Am J Pathol 2000, 156:15–20

27. LaFerla FM, Troncoso JC, Strickland DK, Kawas CH, Jay G: Neuronal cell death in Alzheimer's disease correlates with apoE uptake and intracellular Abeta stabilization. J Clin Invest 1997, 100:310–320

28. Gyure KA, Durham R, Stewart WF, Smialek JE, Troncoso JC: Intraneuronal abeta-amyloid precedes development of amyloid plaques in Down syndrome. Arch Pathol Lab Med 2001, 125:489–492

29. Mori C, Spooner ET, Wisniewsk KE, Wisniewski TM, Yamaguch H, Saido TC, Tolan DR, Selkoe DJ, Lemere CA: Intraneuronal Abeta42 accumulation in Down syndrome brain. Amyloid 2002, 9:88–102

30. Wirths O, Multhaup G, Czech C, Blanchard V, Moussaoui S, Tremp G, Pradier L, Beyreuther K, Bayer TA: Intraneuronal Abeta accumulation precedes plaque formation in beta-amyloid precursor protein and presenilin-1 double-transgenic mice. Neurosci Lett 2001, 306:116–120

31. Chui DH, Tanahashi H, Ozawa K, Ikeda S, Checler F, Ueda O, Suzuki H, Araki W, Inoue H, Shirotani K, Takahashi K, Gallyas F, Tabira T: Transgenic mice with Alzheimer presenilin 1 mutations show accelerated neurodegeneration without amyloid plaque formation. Nat Med 1999, 5:560–564

32. Oddo S, Caccamo A, Shepherd JD, Murphy MP, Golde TE, Kayed R, Metherate R, Mattson MP, Akbari Y, LaFerla FM: Triple-transgenic model of Alzheimer's disease with plaques and tangles: intracellular Abeta and synaptic dysfunction. Neuron 2003, 39:409–421

33. Zhang Y, McLaughlin R, Goodyer C, LeBlanc A: Selective cytotoxicity of intracellular amyloid beta peptide1-42 through p53 and Bax in cultured primary human neurons. J Cell Biol 2002, 156:519–529

34. Kim HJ, Chae SC, Lee DK, Chromy B, Lee SC, Park YC, Klein WL, Krafft GA, Hong ST: Selective neuronal degeneration induced by soluble oligomeric amyloid beta protein. EMBO J 2003, 17:118–120

35. Nakano Y, Kondoh G, Kudo T, Imaizumi K, Kato M, Miyazaki JI, Tohyama M, Takeda J, Takeda M: Accumulation of murine amyloid-beta42 in a gene-dosage-dependent manner in PS1 'knock-in' mice. Eur J Neurosci 1999, 11:2577–2581

36. Baumeister R, Leimer U, Zweckbronner I, Jakubek C, Grunberg J, Haass C: Human presenilin-1, but not familial Alzheimer's disease (FAD) mutants, facilitate Caenorhabditis elegans Notch signalling independently of proteolytic processing. Genes Funct 1997, 1:149–159

37. Saura CA, Choi SY, Beglopoulos V, Malkani S, Zhang D, Shankaranarayana Rao BS, Chattarji S, Kelleher III RJ, Kandel ER, Duff K, Kirkwood A, Shen J: Loss of presenilin function causes impairments of memory and synaptic plasticity followed by age-dependent neurodegeneration. Neuron 2004, 42:23–36

38. Saido TC, Iwatsubo T, Mann DM, Shimada H, Ihara Y, Kawashima S: Dominant and differential deposition of distinct beta-amyloid peptide species, A beta N3(pE), in senile plaques. Neuron 1995, 14:457–466

39. Russo C, Schettini G, Saido TC, Hulette C, Lippa C, Lannfelt L, Ghetti B, Gambetti P, Tabaton M, Teller JK: Presenilin-1 mutations in Alzheimer's disease. Nature 2000, 405:531–532

40. Saido TC, Yamao-Harigaya W, Iwatsubo T, Kawashima S: Amino- and carboxyl-terminal heterogeneity of beta-amyloid peptides deposited in human brain. Neurosci Lett 1996, 215:173–176

41. Russo C, Saido TC, DeBusk LM, Tabaton M, Gambetti P, Teller JK: Heterogeneity of water-soluble amyloid beta-peptide in Alzheimer's disease and Down's syndrome brains. FEBS Lett 1997, 409:411–416

42. Tekirian TL, Saido TC, Markesbery WR, Russell MJ, Wekstein DR, Patel E, Geddes JW: N-terminal heterogeneity of parenchymal and cerebrovascular Abeta deposits. J Neuropathol Exp Neurol 1998, 57:76–94

43. Harigaya Y, Saido TC, Eckman CB, Prada CM, Shoji M, Younkin SG: Amyloid beta protein starting pyroglutamate at position 3 is a major component of the amyloid deposits in the Alzheimer's disease brain. Biochem Biophys Res Commun 2000, 276:422–427

44. Vassar R, Bennett BD, Babu-Khan S, Kahn S, Mendiaz EA, Denis P, Teplow DB, Ross S, Amarante P, Loeloff R, Luo Y, Fisher S, Fuller J, Edenson S, Lile J, Jarosinski MA, Biere AL, Curran E, Burgess T,

Louis JC, Collins F, Treanor J, Rogers G, Citron M: Beta-secretase cleavage of Alzheimer's amyloid precursor protein by the transmembrane aspartic protease BACE. Science 1999, 286:735–741

45. Liu K, Doms RW, Lee VM: Glu11 site cleavage and N-terminally truncated A beta production upon BACE overexpression. Biochemistry 2002, 41:3128–3136

46. Huse JT, Liu K, Pijak DS, Carlin D, Lee VM, Doms RW: Beta-secretase processing in the trans-Golgi network preferentially generates truncated amyloid species that accumulate in Alzheimer's disease brain. J Biol Chem 2002, 277:16278–16284

47. Hebert SS, Bourdages V, Godin C, Ferland M, Carreau M, Levesque G: Presenilin-1 interacts directly with the beta-site amyloid protein precursor cleaving enzyme (BACE1). Neurobiol Dis 2003, 13:238–245

48. Hattori C, Asai M, Oma Y, Kino Y, Sasagawa N, Saido TC, Maruyama K, Ishiura S: BACE1 interacts with nicastrin. Biochem Biophys Res Commun 2002, 293:1228–1232